

## $\rho^0$ Meson Production in the $pp \rightarrow pp\pi^+\pi^-$ Reaction at 3.67 GeV/c

F. Balestra,<sup>1</sup> Y. Bedfer,<sup>2,\*</sup> R. Bertini,<sup>1,2</sup> L. C. Bland,<sup>3</sup> A. Brenschede,<sup>4</sup> F. Brochard,<sup>2,†</sup> M. P. Bussa,<sup>1</sup> Seonho Choi,<sup>3,‡</sup> M. L. Colantoni,<sup>1</sup> R. Dressler,<sup>6,§</sup> M. Dzemidzic,<sup>3,||</sup> J.-Cl. Faivre,<sup>2,\*</sup> A. Ferrero,<sup>1</sup> L. Ferrero,<sup>1</sup> J. Foryciarz,<sup>5,9,¶</sup> I. Fröhlich,<sup>4</sup> V. Frolov,<sup>7,\*\*</sup> R. Garfagnini,<sup>1</sup> A. Grasso,<sup>1</sup> S. Heinz,<sup>1,2</sup> W. W. Jacobs,<sup>3</sup> W. Kühn,<sup>4</sup> A. Maggiora,<sup>1</sup> M. Maggiora,<sup>1</sup> A. Manara,<sup>1,2</sup> D. Panzneri,<sup>8</sup> H.-W. Pfaff,<sup>4,††</sup> G. Piragino,<sup>1</sup> A. Popov,<sup>7</sup> J. Ritman,<sup>4</sup> P. Salabura,<sup>5</sup> V. Tchalyshev,<sup>7</sup> F. Tosello,<sup>1</sup> S. E. Vigdor,<sup>3</sup> and G. Zosi<sup>1</sup>

(DISTO Collaboration)

<sup>1</sup>*Dipartimento di Fisica "A. Avogadro" and INFN, Torino I-10125, Italy*

<sup>2</sup>*Laboratoire National Saturne, CEA, Saclay F-91191, France*

<sup>3</sup>*Indiana University Cyclotron Facility, Bloomington, Indiana 47408*

<sup>4</sup>*II. Physikalisches Institut, University of Gießen, Gießen D-35392, Germany*

<sup>5</sup>*M. Smoluchowski Institute of Physics, Jagellonian University, Kraków 30-059, Poland*

<sup>6</sup>*Forschungszentrum Rossendorf, Rossendorf D-01314, Germany*

<sup>7</sup>*JINR, Dubna 141980, Russia*

<sup>8</sup>*Universita' del Piemonte Orientale and INFN, Torino I-15100, Italy*

<sup>9</sup>*H. Niewodniczanski Institute of Nuclear Physics, Kraków 31-342, Poland*

(Received 18 December 2001; published 12 August 2002)

Total and differential cross sections for the exclusive reaction  $pp \rightarrow pp\rho$  observed via the  $\pi^+\pi^-$  decay channel have been measured at  $p_{\text{beam}} = 3.67$  GeV/c. The observed total meson production cross section is determined to be  $(23.4 \pm 0.8 \pm 8)$   $\mu\text{b}$  and is significantly lower than typical cross sections used in model calculations for heavy-ion collisions. The differential cross sections measured indicate a strong anisotropy ( $\sim \cos\theta_{\rho}^{CM}$ ) in the  $\rho^0$  meson production.

DOI: 10.1103/PhysRevLett.89.092001

PACS numbers: 14.40.Cs, 13.75.Cs, 25.40.Ve

The study of the production of vector mesons (such as  $\rho^0$ ) in both hadronic and electromagnetic processes is considered an excellent tool to investigate the properties of the hadrons both inside the nuclear medium and in free space. These properties are closely related to the QCD vacuum structure characterized by the presence of a non-vanishing quark condensate breaking chiral symmetry [1]. In QCD inspired models, in-medium  $\rho^0$  mass modifications have been proposed as a signal for chiral symmetry restoration in dense and/or hot baryonic matter [1]. Based on these calculations, sizable changes in the  $\rho^0$  spectral function have been predicted for near-threshold  $\rho^0$  production in proton-, pion-, and nucleus-nucleus reactions [2,3]. Furthermore, modifications of the in-medium  $\rho^0$  spectral functions can also rise from  $\rho - N$  coupling as indicated by hadronic model calculations [4,5]. Such modifications could have a significant impact on the role of the  $\rho^0$  as one of the mediators of the nuclear force at small distance, mainly in the tensor part of the interaction [6,7].

A measurement of the  $\rho$  production cross sections in  $pp$  collisions close to threshold is of particular importance for the understanding of the  $\rho - N$  coupling. Unfortunately, the large  $\rho$  width  $\Gamma = 0.15$  GeV/c<sup>2</sup> and a small cross section hampered up to now successful  $\rho^0$  identification for excess energies above threshold  $\epsilon \leq 1.1$  GeV [8]. In this Letter, we report on the first measurement of the exclusive total and differential cross sections of the  $\rho^0$

production in proton-proton reactions at  $\epsilon = 0.33$  GeV, measured at the SATURNE II facility at Saclay.

The proton beam of momentum 3.67 GeV/c was incident on a liquid hydrogen target, and charged particles were detected using the DISTO spectrometer, which is described in detail elsewhere [9]. This spectrometer consisted of a large dipole magnet (40 cm gap size, operating at 1.0 T · m) which covered the target, located at the center, as well as two sets of scintillating fiber hodoscopes. Outside the magnetic field, two sets of multiwire proportional chambers were mounted, along with segmented plastic scintillator hodoscopes (SH) and water Čerenkov detectors (ČD) for particle identification.

The acceptance of all detectors ( $\approx 2^\circ$  to  $\approx 48^\circ$  horizontally and  $\approx \pm 15^\circ$  vertically) on both sides of the beam allowed coincident detection of four charged particles with sizable efficiency. The multiparticle trigger, which was based on the multiplicity of SH elements and the scintillating fibers, selected events with at least three charged tracks in the final state. With this trigger many exclusive channels, e.g.,  $ppK^+K^-$ ,  $pp\pi^+\pi^-\pi^0$  [10–12] and  $pK\Lambda$ ,  $pK\Sigma$  [13] were simultaneously measured.

The exclusive  $\rho^0$  meson production ( $pp \rightarrow pp\rho^0$ ) was measured via its dominant ( $\sim 100\%$ )  $\pi^+\pi^-$  decay channel. Proton and pion identification was achieved by means of conditions defined on two-dimensional distributions of particle momentum versus Čerenkov light and energy loss

measurements in the  $\check{C}D$  and the SH, respectively. It was found that less than 10% of the pions could be misidentified protons. The selection of the  $pp \rightarrow pp\pi^+\pi^-$  reaction was based on two kinematical conditions that were checked with Monte Carlo simulations: (a) the four particle missing mass has to be zero  $(M_{4p}^{\text{miss}})^2 = 0 \pm 0.015 \text{ GeV}^2/c^4$ , and (b) the proton-proton missing mass has to be equal to the  $\pi^+\pi^-$  invariant mass  $(M_{pp}^{\text{miss}})^2 = (M_{\pi^+\pi^-}^{\text{inv}})^2 \pm 0.2 \text{ GeV}^2/c^4$ . The residual background below the  $(M_{pp}^{\text{miss}})^2$  bump amounts to only about 2% of the total yield and can mainly be attributed to events from the  $pp\pi^+\pi^-\pi^0$  reaction.

The acceptance of the DISTO spectrometer for the  $pp\pi^+\pi^-$  channel was determined using Monte Carlo simulations, which after digitization were processed through the same analysis chain as the measured data. The production of a meson  $X$  with the given mass  $M_X$ , in the exclusive reaction  $pp \rightarrow ppX \rightarrow pp\pi^+\pi^-$ , was assumed for the final state particles generation. Eight linearly independent degrees of freedom are necessary to fully describe a four body final state. We have chosen the following variables:  $(M_{p_1X}^{\text{inv}})^2$ ,  $(M_{p_2X}^{\text{inv}})^2$ , and three Euler angles  $\theta_X^{\text{CM}}$ ,  $\phi_X^{\text{CM}}$ ,  $\psi_{pp}^{\text{CM}}$  in the center of mass frame (CM) that characterize the  $ppX$  system, and  $M_X$ ,  $\theta_\pi^X$ ,  $\phi_\pi^X$  which describe the  $X \rightarrow \pi^+\pi^-$  decay [12]. The spectrometer acceptance has been determined as a four-dimensional function of the variables  $(M_{p_1X}^{\text{inv}})^2$ ,  $(M_{p_2X}^{\text{inv}})^2$ ,  $\theta_X^{\text{CM}}$ , and  $M_X$ , assuming isotropic distributions in the remaining four variables. Symmetry reasons ensure that the distribution of  $\phi_X^{\text{CM}}$  must be isotropic, and the isotropic assumption for the remaining three variables was corroborated by the measured data.

The simulations indicate a very low acceptance of the apparatus for the  $X$  produced in the backward hemisphere in the CM frame. However, since the initial system consists of two identical particles, a reflection symmetry about  $\theta^{\text{CM}} = 90^\circ$  exists; thus the backward data are redundant for the total cross section determination. In the forward hemisphere the detector acceptance was found to be non-zero in every bin over the full kinematically allowed region, thus eliminating the need for any model dependent extrapolations of the cross section into unmeasured regions of phase space. As a result, the acceptance corrections for the DISTO spectrometer are independent of the actual final state distributions, except for residual effects related to the size of the kinematic bins and the detector resolution, which have been accounted for in the estimate of the systematic error. Finally, the data presented below have been corrected on an event-by-event basis, via a weighting factor obtained from the acceptance function for the appropriate kinematic bin.

Compared to the other mesons identified in our experiment [10–12], the extraction of the  $\rho^0$  yield from the nonresonant background is much more difficult because of its larger width. Therefore, different selection criteria had to be applied. For each of them the effect on the

acceptance for  $\rho^0$  and background events has been evaluated using the Monte Carlo simulation mentioned above. A first selection was applied on the three body  $p\pi^+\pi^-$  invariant mass  $M_{p\pi^+\pi^-}^{\text{inv}} > 1.6 \text{ GeV}/c^2$  for both  $p\pi^+\pi^-$  combinations. It was found that this rejects 35% of the  $pp\pi^+\pi^-$  events, whereas the simulations indicate that only less than 4% of  $\rho^0$  events are lost by this restriction.

A further investigation of the remaining events shows that, as observed at higher energies [8], most two pion events originate from the  $pp \rightarrow \Delta^{++}p\pi^-$  channel. Figure 1 shows the acceptance corrected  $p\pi^+$  invariant mass distributions for events fulfilling the  $M_{p\pi^+\pi^-}^{\text{inv}} > 1.6 \text{ GeV}/c^2$  condition discussed above. The  $M_{p_1\pi^+}^{\text{inv}}$  and  $M_{p_2\pi^+}^{\text{inv}}$  have been obtained, selecting the events according to the absolute value of the four-momentum transfer  $|t|$ , from the incoming beam proton to the outgoing  $p\pi^+$  system.  $M_{p_1\pi^+}^{\text{inv}}$  and  $M_{p_2\pi^+}^{\text{inv}}$  denote the invariant mass of the  $p\pi^+$  pair with smaller and larger momentum transfer, respectively. The prominent  $\Delta^{++}$  peak at  $M_{p\pi^+}^{\text{inv}} = 1.231 \pm 0.008 \text{ GeV}/c^2$  is visible in both distributions. A fit to the data using a relativistic Breit-Wigner distribution [3] of width  $\Gamma = 0.12 \text{ GeV}/c^2$  added onto a third order polynomial background shape indicates that 77% of all  $pp\pi^+\pi^-$  events involve  $\Delta^{++}$  production.

In order to reduce the background related to  $\Delta^{++}$  production, it was required that the invariant mass for both  $p\pi^+$  combinations be  $1.15 \text{ GeV}/c^2 < M_{p\pi^+}^{\text{inv}} < 1.28 \text{ GeV}/c^2$  and that the three body invariant mass  $M_{p_1\pi^+\pi^-}^{\text{inv}} < 1.74 \text{ GeV}/c^2$ . With such conditions 50% of the  $\pi^+\pi^-$  pairs were rejected, whereas the simulation showed that only 10% of those from  $\rho^0$  decay are lost. A similar selection on  $p\pi^-$  invariant mass was judged unnecessary, since events involving  $\Delta^0$  production are much less abundant than those with  $\Delta^{++}$  and therefore will not enhance the  $\rho^0$  signal to background ratio.

For the events surviving all the criteria described above, Fig. 2 presents the final, acceptance corrected  $M_{\pi^+\pi^-}^{\text{inv}}$

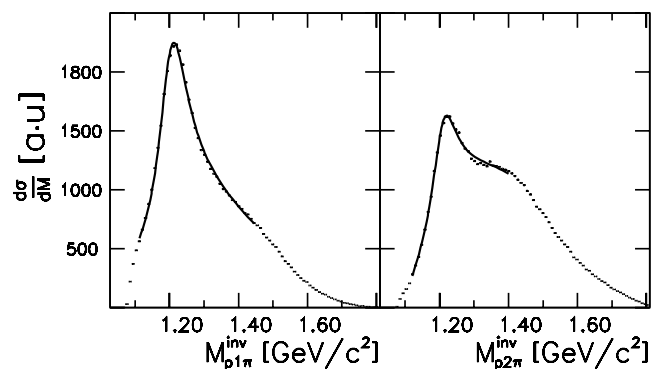


FIG. 1. Proton-pion invariant mass distributions  $M_{p\pi}^{\text{inv}}$  selected according to the absolute value of the four-momentum transfer  $t$ :  $M_{p_1\pi^+}^{\text{inv}}$  with the lower  $|t|$  value (left frame) and  $M_{p_2\pi^+}^{\text{inv}}$  with the larger  $|t|$  (right frame). The curves are fits to the data as explained in the text.

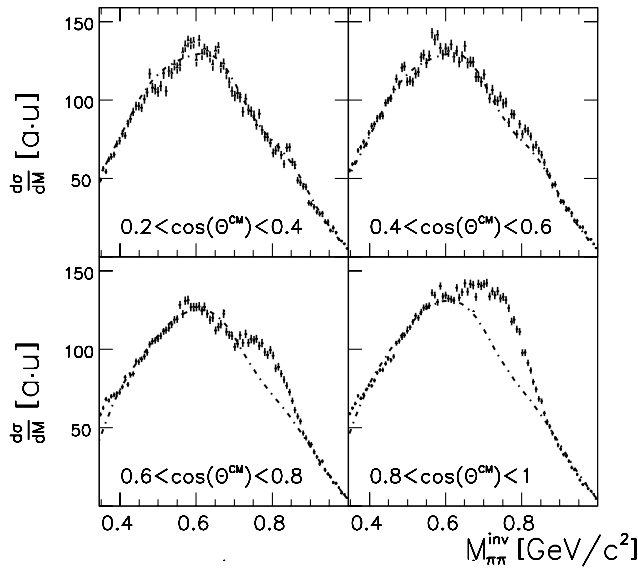


FIG. 2.  $\pi^+\pi^-$  invariant mass distributions obtained in four different CM angular bins as indicated in the figure. The dashed line represents the smoothed invariant mass distribution for the  $0 < \cos(\theta^{\text{CM}}) < 0.2$  normalized to the maximum.

distributions for four equal bins in  $\cos(\theta^{\text{CM}})$  between  $\cos(\theta^{\text{CM}}) = 0.2$  and  $\cos(\theta^{\text{CM}}) = 1.0$ , where  $\theta^{\text{CM}}$  is the CM polar emission angle of the di-pion system with respect to the beam axis. The dashed line shows the smoothed  $M_{\pi^+\pi^-}^{\text{inv}}$  distribution for  $0 < \cos(\theta^{\text{CM}}) < 0.2$  normalized to the maximum, which reproduces well the general shape of the  $\pi^+\pi^-$  nonresonant spectra. It should be noted that this yield is almost independent of  $\cos(\theta^{\text{CM}})$  indicating a nearly isotropic  $\pi^+\pi^-$  nonresonant production. A structure near the  $\rho^0$  mass  $M_\rho = 0.77 \text{ GeV}/c^2$  is clearly visible.

The  $\rho^0$  yield has been extracted from a fit to the  $M_{\pi^+\pi^-}^{\text{inv}}$  distributions using a function  $\sigma(m) = \text{BW}(m, \Gamma)V_{ps}(m)$  describing the  $\rho^0$  line shape and a third order polynomial background. The  $\text{BW}(m, \Gamma)$  is a relativistic Breit-Wigner function with a mass dependent pion decay width of the meson given by [3]:  $\Gamma = \Gamma(m_R)\left(\frac{k_\pi(m)}{k_\pi(m_R)}\right)^3 \frac{m_R}{m}$ , where  $\Gamma(m_R) = 0.15 \text{ GeV}/c^2$  is the full  $\rho^0$  width at its pole position  $m_R = M_\rho$  and  $k_\pi(m)$ ,  $k_\pi(m_R)$  are pion three-momenta in the rest frame of the resonance with masses  $m$  and  $m_R$ , respectively.  $V_{ps}(m)$  stands for the phase space available for the direct (no intermediate state) production of the meson with a given mass  $m$ . We have calculated  $V_{ps}(m)$  by numerical integration of the simulated  $pp\rho$  Dalitz distribution including the  $\Delta^{++}$  suppression cuts discussed above. As an example, Fig. 3 shows the  $M_{\pi^+\pi^-}^{\text{inv}}$  distribution for  $\cos(\theta^{\text{CM}}) \geq 0.5$  containing most of the  $\rho^0$  yield. The initial background parameters have been obtained by fitting the  $M_{\pi^+\pi^-}^{\text{inv}}$  distribution for  $\cos(\theta^{\text{CM}}) \leq 0.4$  and  $M_{\pi^+\pi^-}^{\text{inv}} \geq 0.55 \text{ GeV}/c^2$  normalized to the same maximum (dashed line). The best fit ( $\chi^2/\nu = 1.2$ ) has been obtained with a fixed  $\Gamma(m_R) = 0.15$ ,  $M_R = 0.772 \pm$

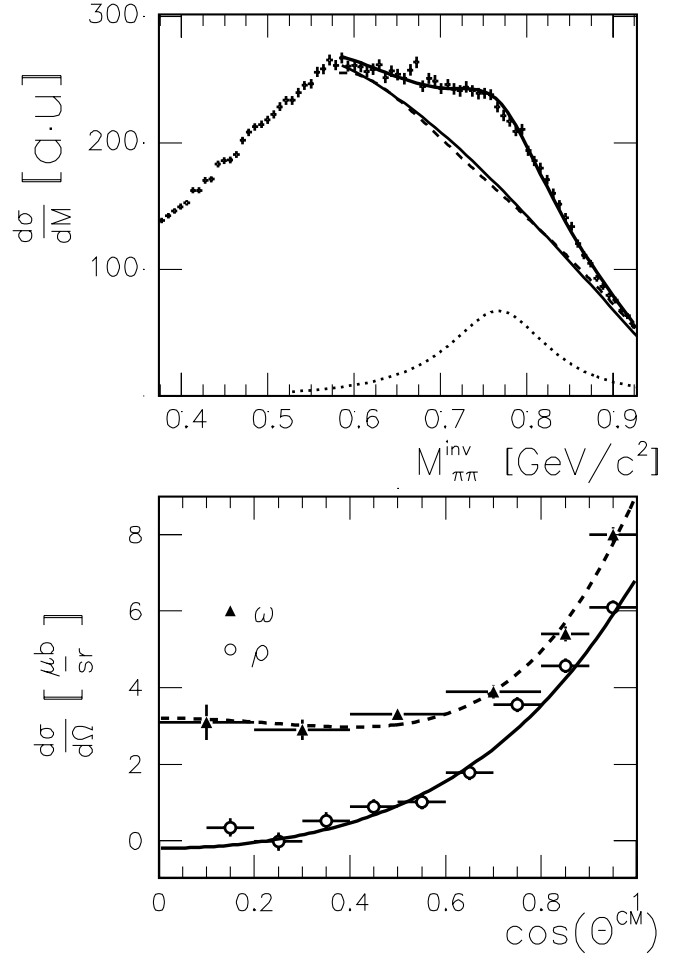


FIG. 3. Upper frame:  $M_{\pi^+\pi^-}$  distribution measured for  $\cos(\theta^{\text{CM}}) > 0.5$ . The solid line shows the fit using a relativistic Breit-Wigner function added onto a third order polynomial for the background, as described in the text. The dotted line shows the meson line shape, and the dashed line presents the  $M_{\pi^+\pi^-}^{\text{inv}}$  distribution obtained for  $\cos(\theta^{\text{CM}}) < 0.4$  normalized to the same maximum. Lower frame: The  $\rho^0$  (circles) and  $\omega$  (triangles) differential cross sections as a function of the meson CM emission polar angle. The solid and dashed lines show fits using the first three even Legendre polynomials.

$0.003 \text{ GeV}/c^2$  (dotted line), and background (solid line) which differs only very little from its initial shape.

In order to extract the angular distribution for the  $\rho^0$  production and to extract the total production yield, a finer angular bin size was chosen, and the fit procedure outlined above has been applied. The total  $\rho^0$  yield has been obtained as a sum of yields in the individual angular bins. The total cross section of  $\sigma = (23.4 \pm 0.8 \pm 8) \mu\text{b}$  with statistical and systematic errors, respectively, was determined by normalizing the acceptance corrected  $\rho^0$  yield to the simultaneously measured exclusive  $\eta$  yield of known cross section  $\sigma_\eta = 135 \pm 35 \mu\text{b}$ . The  $\eta$  yield was obtained using separate acceptance correction matrices but calculated with the same method [12]. This procedure to determine the absolute normalization was chosen because it

reduced the large systematic uncertainty associated with the determination of the absolute beam intensity and trigger efficiency. It was checked by detailed Monte Carlo simulations that particle identification efficiencies and yield reductions due to the analysis cuts applied for the selections of various reactions are understood within 15% [12]. Finally, the method was verified by comparing the exclusive cross section for  $\omega$  production measured in our experiment [12] with other experimental results obtained in a similar energy range. An interpolation between existing data points give  $\sigma_\omega = 45 \pm 7 \mu\text{b}$  [14] in good agreement with our result  $\sigma_\omega = 50 \pm 3_{-16}^{+18} \mu\text{b}$ .

The systematic uncertainty for the  $\rho^0$  cross section contains two almost equal contributions: (a) errors from absolute normalization and (b) uncertainties related to the background subtraction, acceptance corrections, tracking efficiency, and analysis cuts. In particular, a possible bias in the analysis due to the  $\Delta^{++}$  suppression has been investigated by comparing the  $\rho^0$  intensity obtained with and without the suppression. The observed yield reduction of  $\sim 10\%$  was reproduced by the Monte Carlo simulations mentioned above, was corrected for, and was completely included in the systematic errors.

Polar angle differential cross sections have been proposed [15] as a sensitive observable to extract the strength of nucleonic and mesonic currents responsible in meson exchange models for the vector meson production near the threshold. Therefore, it is particularly interesting for various reaction models to compare the differential cross sections for the production of  $\rho^0$  and  $\omega$  as measured in our experiment [12]. The lower part of Fig. 3 shows the  $\rho^0$  (circles) and  $\omega$  (triangles) production cross section as a function of  $\cos\theta^{\text{CM}}$ , the polar angle in the CM system of the meson. The vertical error bars reflect the statistical errors only. The distributions have been fit with the sum of the first three Legendre polynomials (solid line)  $P_i$  with the result  $\frac{d\sigma_\rho}{d\Omega} \propto (2. \pm 0.2)P_0 + (4.4 \pm 0.2)P_2 + (0.8 \pm 0.2)P_4$  and  $\frac{d\sigma_\omega}{d\Omega} \propto (4 \pm 0.1)P_0 + (3.1 \pm 0.2)P_2 + (2.0 \pm 0.2)P_4$  for the  $\rho^0$  and  $\omega$ , respectively.

The above results indicate a contribution of partial waves up to  $L = 2$  in the production of both mesons. Clearly, the angular distribution for  $\rho^0$  production exhibits stronger forward peaking, suggesting a dominance of the nucleonic current characterized by a dipole  $\sim \cos^2\theta^{\text{CM}}$  dependence [15]. The angular distributions for  $\omega$  production at this beam energy and at the smaller excess energy  $\epsilon = 0.173 \text{ GeV}$  [16] show strong nucleonic contribution too, but also an additional isotropic component signaling the importance of the mesonic  $\pi\rho \rightarrow \omega$  fusion [15]. It is also interesting to note that the observed ratio of the total cross sections for  $\rho^0$  and  $\omega$  production  $R = \sigma(\rho^0)/\sigma(\omega) = 0.46 \pm 0.12$  is very similar to the ratio obtained at higher energy ( $\epsilon = 1.14 \text{ GeV}$ )  $R =$

$0.48 \pm 0.13$  [8] and seems to indicate similar scaling of the cross section with  $\sqrt{s}$  for both mesons.

In conclusion, the production of the  $\rho^0$  meson has been studied in the  $pp$  reaction at  $p_{\text{beam}} = 3.67 \text{ GeV}/c$ . A total  $\rho^0$  cross section of  $\sigma = (23.4 \pm 0.8 \pm 8) \mu\text{b}$  has been determined. It is significantly lower than typical cross sections used by the hadronic models ( $\sim 100 \mu\text{b}$ ) for meson production in pA and AA collisions [3,17]. Furthermore, the differential cross sections exhibit a prominent  $\frac{d\sigma_\rho}{d\Omega} \propto \cos^2\theta^{\text{CM}}$  dependence that might signal the dominance of nucleonic current in  $\rho^0, \omega$  meson production.

We thank the SATURNE II staff for delivering an excellent proton beam and for assisting this experimental program. This work has been supported by CNRS-IN2P3, CEA-DSM, NSF, INFN, KBN (5P03B14020), and GSI.

---

\*Present address: DAPNIA/SPhN, CEA Saclay, France.

†Present address: LPHNHE, Ecole Polytechnic, 91128 Palaiseau, France.

‡Present address: Temple University, Philadelphia, PA.

§Present address: Paul Scherrer Institut, Villigen, CH-5232.

||Present address: IU School of Medicine, Indianapolis, IN.

¶Present address: Motorola Polska Software Center, Kraków, Poland.

\*\*Present address: Dip. di Fisica "A. Avogadro" and INFN-Torino, Italy.

††Present address: Arthur Andersen, Eschborn, Germany.

- [1] G. E. Brown and M. Rho, Phys. Rev. Lett. **66**, 2720 (1991).
- [2] G. Q. Li, C. M. Ko, and G. E. Brown, Phys. Rev. Lett. **75**, 4007 (1995).
- [3] W. Cassing and E. L. Bratkovskaya, Phys. Rep. **308**, 65 (1999).
- [4] R. Rapp and J. Wambach, Adv. Nucl. Phys. **25**, 1 (2000).
- [5] W. Peters *et al.*, Nucl. Phys. **A632**, 109 (1998); B. Friman and H. Pinner, Nucl. Phys. **A617**, 496 (1997).
- [6] R. Machleidt, Adv. Nucl. Phys. **19**, 189 (1989).
- [7] D. Jido, E. Oset, and J. E. Palomar, nucl-th/0202070.
- [8] G. Alexander *et al.*, Phys. Rev. **154**, 1284 (1967); E. Colton *et al.*, Phys. Rev. D **3**, 1063 (1971).
- [9] F. Balestra *et al.*, Nucl. Instrum. Methods Phys. Res., Sect. A **426**, 385 (1999).
- [10] F. Balestra *et al.*, Phys. Rev. Lett. **81**, 4572 (1998).
- [11] F. Balestra *et al.*, Phys. Lett. B **468**, 7 (1999).
- [12] F. Balestra *et al.*, Phys. Rev. C **63**, 024004 (2001).
- [13] F. Balestra *et al.*, Phys. Rev. Lett. **83**, 1534 (1999).
- [14] A. Sibirtsev and W. Cassing, Eur. Phys. J. A **7**, 407 (2000).
- [15] K. Nakayama *et al.*, Phys. Rev. C **57**, 1580 (1998).
- [16] S. Abd El-Samad *et al.*, Phys. Lett. B **522**, 16 (2001).
- [17] S. Teis *et al.*, Z. Phys. A **356**, 421 (1997); C. Ernst *et al.*, Phys. Rev. C **58**, 447 (1998); E. L. Bratkovskaya, Nucl. Phys. **A653**, 301 (1999).